Ti and Si doping as a way to increase low temperature activity of sulfated Ag/Al_2O_3 in H_2-assisted NH_3-SCR of NO_x

Dmitry E. Doronkin[1,2], Sebastian Fogel[2,3], Pär Gabrielsson[3], Jan-Dierk Grunwaldt[1], Søren Dahl[2,3]*

[1]Institut für Technische Chemie und Polymerchemie, Karlsruher Institut für Technologie (KIT), Engesserstr. 20, 76131 Karlsruhe, Germany

[2]Center for Individual Nanoparticle Functionality (CINF), Department of Physics, Technical University of Denmark, Fysikvej 307, 2800 Kgs. Lyngby, Denmark

[3]Haldor Topsøe A/S, Nymøllevej 55, 2800 Kgs. Lyngby, Denmark

[*] Corresponding author: tel.: +49 721 608 48090, e-mail: *dmitry.doronkin@kit.edu*

Abstract

Ag/Al_2O_3 catalysts modified by Si, Ti, Mg and W were studied to obtain higher NO_x SCR activity and potentially also higher SO_2 resistance than the pure silver-based catalyst for automotive applications. Addition of Ti or Si to the alumina support leads to a better NO_x removal at low temperature i.e. reduces the SCR onset temperature by about 10 °C under the applied conditions. However, it does not increase the SO_2 resistance. The catalysts and the supports have been characterized by BET, conventional and synchrotron XRD, X-ray absorption spectroscopy during temperature-programmed reduction (XAS-TPR) and temperature-programmed desorption of ammonia (NH_3-TPD). The obtained results suggest a better silver dispersion and better regeneration capability in the case of Ti- and Si-modified Ag/Al_2O_3 catalysts.

Keywords: Ag/Al_2O_3; doping; NO_x SCR; sulphur tolerance; X-ray absorption spectroscopy

1. Introduction

Light-duty diesel engines require removal of nitrogen oxides (NO_x) from the exhaust at temperatures below 200 °C to meet the upcoming emission legislation [1]. Among commercial selective catalytic reduction (SCR) catalysts only Cu-zeolites have been reported to achieve high NO_x conversion at so low temperatures [2]. However, these catalysts are prone to sulfur poisoning [3] and until recently to severe hydrothermal deactivation [4]. There are other low-temperature NO_x removal systems including lean NO_x traps (LNT), combinations of LNT and SCR catalysts which utilize the ”Fast SCR” effect [5-8] under development.

Ag/Al_2O_3 catalysts allow NO_x conversion by ammonia up to 90% at 200 °C provided hydrogen is co-fed [9,10]. However, sulfur tolerance of the catalyst still remains an issue [11] that may be overcome by supply of an excess of hydrogen [10]. However, currently, that it is economically not viable.

An alternative way to increase the sulfur tolerance of Ag/Al_2O_3 is a modification of the catalyst itself. Park and Boyer [12] observed increased stability using higher Ag loading in the catalyst. Instead of the commonly used $2\%Ag/Al_2O_3$ catalyst they applied $8\%Ag/Al_2O_3$ for NO_x SCR by hydrocarbons (HC-SCR). Kumar et al. [13] suggested alumina modification by 1-5%Mg which resulted in increased catalytic activity and stability of Ag/Al_2O_3 in the presence of 80 ppm SO_2 during the same process. C.N. Costa with coauthors [14] suggested using $0.1\%Ag/MgO\text{-}CeO_2\text{-}Al_2O_3$ as a highly active catalyst stable towards sulfur for NO_x SCR by ethanol. Li et al. [15] observed a great enhancement of NO_x SCR by propene over a $5\%Ag/TiO_2–Al_2O_3$ catalyst compared to $5\%Ag/Al_2O_3$, which they attributed to a better Ag dispersion due to the modified support. Moreover, this catalyst showed a slower rate of sulfate accumulation than the

reference. Similar observation has been made in another study [16] where a 2%Ag/Al_2O_3 catalyst was doped by 1%SiO_2 or 1%TiO_2 (via impregnation of Al_2O_3 with Si and Ti precursors). Together with a slight decrease in NO_x conversion by propene a significant increase in SO_2 tolerance was demonstrated for the doped catalysts. Finally, Nb-doping of Ag/Al_2O_3 was shown to increase conversion of NO_x at low temperatures [17].

In a previous study we showed the existence of different Ag sites with different SO_2 tolerance [18] which explained the importance of having a relatively high Ag load on high surface area alumina, e.g. 4-6%Ag / 250-300m^2/g Al_2O_3 to obtain the most SO_2 tolerant catalyst [19].

In the current study 6%Ag/Al_2O_3 catalyst was modified by loading Ti, Si, Mg, and W. Our goal was to improve the stability and activity of Ag/Al_2O_3 for the H_2-assisted NO_x SCR by NH_3 and unravel the influence of the dopants both by catalytic and characterization studies.

2. Experimental

2.1. Catalyst preparation

Parent γ-alumina (S_{BET}=298 m^2/g) was prepared via calcination of pseudoboehmite at 500 °C for 4h in static air.

For the Ti/Al_2O_3 and the Si/Al_2O_3 the corresponding dopants were deposited on the alumina by an incipient wetness impregnation with titanium (IV) isopropoxide (Aldrich) and TEOS (Tetraethyl orthosilicate, Aldrich) in butanol, respectively. 1%Mg/Al_2O_3 was obtained by incipient wetness impregnation with an aqueous solution of $Mg(NO_3)_2$ (Aldrich). 0.9%W/Al_2O_3 was prepared by two consecutive impregnations

with an aqueous solution of ammonium metatungstate $(NH_4)_6H_2W_{12}O_{40}$ (Aldrich). After impregnation the materials were dried at room temperature overnight and calcined at 550 °C for 4 h in static air.

Commercially available silica-alumina (Siralox 5/230, 5 mol.% SiO_2, 95 mol.% Al_2O_3, S_{BET}=292 m^2/g) containing approx. 3 wt.% Si was also tested as a catalyst support to check whether the results of the laboratory doped aluminas are transferable to the case of the commercial co-precipitated silica-aluminas. The material was kindly supplied by SASOL, Germany.

6% Ag was introduced by an incipient wetness impregnation of the obtained supports with an aqueous solution of $AgNO_3$ (Aldrich). After impregnation all catalysts were dried overnight and calcined at 550 °C for 4 h in static air.

As a final step the catalysts (except Ag/Siralox and Ag/Al_2O_3-noSO_x) were presulfated to increase NO_x conversion at intermediate temperatures (the same effect as observed in ref. [12]). For this purpose, the catalysts were impregnated with an aqueous solution of $(NH_4)_2SO_3$ (Aldrich) and dried at room temperature. 1 g of catalyst required 0.036 g of ammonium sulfite.

The catalysts were denoted $Ag/xXX/Al_2O_3$, where XX is the dopant and x stands for a weight loading of the dopant if any, e.g. a catalyst doped with 1 wt.% Si is denoted as $Ag/1Si/Al_2O_3$.

The catalyst prepared on the basis of the commercial silica-alumina was denoted Ag/Siralox. This catalyst was also studied by synchrotron-XRD and X-ray absorption spectroscopy during temperature-programmed reduction (XAS-TPR). For comparison purpose an unsulfated undoped Ag/Al_2O_3 (Ag/Al_2O_3-noSO_x) reference material was prepared and characterized.

A catalyst 1Ti/Ag/Al_2O_3 was also prepared to check if it is possible to load Ag before loading the dopant (Ti). All the preparation stages were the same as described above.

For catalytic measurements the catalysts were pressed, crushed and sieved to obtain the fraction 0.18 – 0.35 mm (mesh 80 – mesh 45).

2.2. Catalytic experiments

The catalytic measurements were carried out in a fixed-bed quartz flow reactor (inner diameter = 4 mm) in a temperature programmed mode while the temperature was decreased from 400 °C to 150 °C with a rate of 2 °C/min. The temperature was controlled using an Eurotherm 2416 temperature controller with a K-type thermocouple. 45 mg of catalyst was diluted with 100 mg of SiC (mesh 60) and placed on a quartz wool bed. The bed height was ~11mm and the GHSV, calculated using the volume of the pure catalyst was ~ 110 000 h^{-1}. The gas composition normally contained 500 ppm NO, 520 ppm NH_3, 1200 ppm of H_2, 8.3% O_2, and 7% water balanced with Ar. The gas feed was mixed from 2000 ppm NO in Ar, 2000 ppm NH_3 in Ar, 4000 ppm H_2 in Ar (Air Liquide), oxygen and argon (AGA), dosed by individual mass flow controllers (UNIT Celerity). Water was dosed by an ISCO 100DM syringe pump through a heated capillary. Reaction products were analyzed by a Thermo Fisher Nicolet 6700 FTIR analyzer equipped with a 2m gas cell. Gas capillaries were heated to ~130 °C and the FTIR gas cell to 165 °C to avoid condensation of water and formation of ammonium nitrate.

NO_x conversions were calculated using the following equation:

$$X_{NOx} = 1 - \frac{C_{NOx}^{outlet}}{C_{NOx}^{inlet}} \quad (1)$$

where X_{NOx} denotes total conversion of NO_x and C_{NOx}^{inlet} and C_{NOx}^{outlet} is the NO_x concentrations on the inlet and outlet of the reactor, where:

$$C_{NOx} = C_{NO} + C_{NO_2} + C_{N_2O} \ . \qquad (2)$$

Ammonia conversion was calculated accordingly and below 350 °C (the region of interest) corresponds well to NO_x conversion.

For catalyst "degreening" (i.e. bringing its performance in the presence of poisoning agents such as SO_2 to a steady-state level) the samples were heated to 250 °C where 10 ppm SO_2 was introduced and the activity measurement started. After 2 h at 250 °C SO_2 was switched off and the temperature was increased to 670 °C and held there for 15 min before cooling to 250 °C again. Then the cycle, 2 h at 250 °C followed by 15 min at 670 °C, was repeated 7 times (until no difference in activity between the two last sulfation cycles could be seen).

2.3. Catalyst characterization

Temperature programmed desorption (TPD) of NH_3 was conducted in the catalyst test setup (see above) and with the same amount of catalyst (45 mg). Prior to the experiment, the parent unsulfated catalyst support was pretreated in a flow of Ar (100 ml/min) for 30 min at 500°C. After that the sample was cooled down, NH_3 was then adsorbed at 90°C (monitored by FTIR), followed by a switch back to Ar flow to remove gaseous NH_3. When the NH_3 signal was below 10 ppm the temperature ramp was started (5 °C/min).

The specific surface areas (S_{BET}) of the supports were measured by N_2-adsorption with a Micromeritics Gemini instrument. 5-point BET curve was used for S_{BET} determination.

The crystal phase of the materials was investigated by X-ray diffraction (XRD) on a PANalytical X'Pert PRO diffractometer using a Cu K_α radiation (2Θ range 30 – 90°, 45 min per scan).

2.4. Synchrotron X-ray absorption spectroscopy and diffraction studies

The synchrotron studies were performed at the Swiss-Norwegian Beamline (BM01B) at the ESRF synchrotron radiation source. The storage ring typically operates at 6 GeV and injection currents of 200 mA in a top-up mode. For the synchrotron XRD and XAS in terms of X-ray absorption near edge structure (XANES) and extended X-ray absorption fine structure (EXAFS) spectroscopy during TPR the two catalysts Ag/Al_2O_3-noSO_x and Ag/Siralox were placed in 1.5 mm quartz capillaries [20] with 0.01 mm thick walls (approx. 1 cm bed length, 7 mg of a catalyst, sieve fraction 100 – 200 µm). The capillary was placed across the X-ray beam on top of a hot air blower (Oxford GSB-1300) [21] and the capillary was glued with epoxy resin into a special home made holder connected to the inlet and outlet gas lines [22]. Catalyst was heated from 20 to 480°C with 5 °C/min ramp in a flow of 5%H_2 in He (50 ml/min).

XRD patterns were recorded at 24.538 keV (λ = 0.50527 Å) using a 2D-detector (Dexela 2D CMOS) and converted to XY-format using FIT2D software from ESRF [23]. The beam size for XRD was 1x1 mm and the exact X-ray wavelength was determined by measuring a LaB_6 reference. The baseline for the individual peaks of Ag metal and Ag_2O was defined by a linear equation in the 2θ ranges 12.1 – 12.45° and 23.2 – 24° correspondently.

X-ray absorption spectra were recorded in transmission geometry with a Si(111) double-crystal monochromator and a gold-coated mirror for the rejection of higher

harmonics. Three ionization chambers were used for recording the intensities and a third one for an Ag foil used as a standard. Spectra were treated and linear combination analysis was done by using Athena software [24]. For the Fourier transform k^3-weighing and a k-range of 2 – 14 $Å^{-1}$ with Hanning-type window was used. For the linear combination fitting first (oxidized) and last (reduced) spectra were used. The spectra were fit with fixed energy in the range of -10 to +30 eV relative to the threshold energy.

3. Results

3.1. Catalytic activity of Ti, Si, Mg, and W-doped Ag/Al_2O_3

Fig. 1 shows NO_x conversion curves for doped Ag/Al_2O_3 catalysts after degreening. In spite of being an acidic dopant like Ti and Si, addition of 0.9 wt.% W shifted the SCR onset temperature to higher values and significantly decreased the maximum NO_x conversion (gray dashed line). Addition of 1 wt.% Mg, which was effective in the case of HC-SCR [13, 14], did not lead to significant positive changes in the catalytic behavior of $Ag/1Mg/Al_2O_3$ during NH_3-SCR (gray solid line). In the case of $Ag/1.5Ti/Al_2O_3$ (black dashed) and $Ag/1Si/Al_2O_3$ (black dotted) catalysts a shift of the SCR onset to lower temperatures was observed. This 10 °C shift in the range of 150 – 180 °C is important for automotive applications as the exhaust temperature of the light-duty diesel engine is reported to vary between 120 - 190 °C with an average of 142 °C during the urban driving [1].

The same increase in the NO_x conversion was obtained for the Ag/Siralox (gray dotted) which was prepared using the commercial co-precipitated silica-alumina containing approx. 3 wt.% Si. This catalyst was not presulfated as described in 2.1 but

was degreened with SO_2 like all other samples. According to additional previous experiments (not shown), the lack of presulfation in this case influences only the activity of the fresh catalyst but after degreening with SO_2 (section 2.2) the difference disappears.

To evaluate whether the Ag loading and the dopant loading steps can be interchanged, a $1Ti/Ag/Al_2O_3$ catalyst was prepared and compared to its counterpart $Ag/1Ti/Al_2O_3$. The activity profile of $1Ti/Ag/Al_2O_3$ was the same as of reference Ag/Al_2O_3. Thus, the parent alumina support should be doped by Ti or Si as a first step and not the already prepared Ag/Al_2O_3.

Another important parameter of Ag/Al_2O_3 catalysts is their sulfur tolerance. This was evaluated during the degreening procedure which comprised of cycling between 2 h periods with 10 ppm SO_2 at 250 °C and 15 min regeneration periods at 670 °C. The last, 7^{th}, SO_2 poisoning period is shown in Fig. 2 for $Ag/1.5Ti/Al_2O_3$ (black dashed), $Ag/1Si/Al_2O_3$ (black dotted), reference Ag/Al_2O_3 (black solid), and $Ag/1Mg/Al_2O_3$ (gray solid). Ag/Siralox showed similar results to the $Ag/1Si/Al_2O_3$. The data suggests that addition of Mg does not improve the SO_2 tolerance of the Ag/Al_2O_3 catalyst for the NH_3-SCR. Addition of 1 wt.% Si did not change the SO_2 tolerance of the Ag/Al_2O_3 and 1.5 wt.% Ti – slightly decreased the SO_2 tolerance of the Ag/Al_2O_3. Both catalysts preserved a good regeneration capability.

3.2. Dependence of performance of doped Ag/Al_2O_3 on the Ti or Si loading

The optimal amount of Ti and Si in the Ag/Al_2O_3 is governed by the catalyst performance, e.g. SCR onset temperature and sulfur tolerance. Therefore, these parameters were measured for a series of Ti and Si doped samples. Fig. 3 shows the

dependence of SCR onset temperature (shown as temperature of 50% NO_x conversion) on the loading of Ti (circles, solid line) and Si (triangles, dashed line). The best activity is achieved by doping with 1.5 wt.% Ti (0.32 mmol/g) and around 1 wt.% Si (0.36 mmol/g). By loading a higher amount of dopant the catalytic activity decreases significantly, reflected in a higher T_{50} value of the NO_x conversion. Note that the presented results were obtained with dopants loaded on the alumina by impregnation (the dopant mainly stays on the surface) and the optimal loading may differ for co-precipitated titania- and silica-aluminas (where the dopant is evenly distributed in the bulk).

The sulfur tolerance of the degreened Ti- and Si-doped catalysts is presented in Fig. 4 as NO_x conversion at the end of the 120 min sulfation cycle at 250 °C (see 3.1). No increase in NO_x conversion is seen and it even decreases a little with Ti doping suggesting that the main effect of the doping is increasing the low-temperature activity of the regenerated catalyst.

3.3. Temperature programmed desorption of ammonia from Ti- and Si-doped aluminas

To explain the observed increase in the low-temperature activity of $Ag/Ti/Al_2O_3$ and $Ag/Si/Al_2O_3$ we performed physico-chemical studies of the catalysts. The support acidity may influence NO_x SCR by ammonia significantly [25]. Ti and Si are acidic dopants for the alumina [26, 27]. We can, therefore, expect increased acidity of the doped catalysts, which was investigated by temperature programmed desorption of ammonia (NH_3-TPD).

NH_3-TPD profiles of the parent unsulfated 1.5Ti/Al_2O_3 (dashed), 1Si/Al_2O_3 (dotted), and reference Al_2O_3 (solid) are given in Fig. 5 and the amount of acid sites calculated from these profiles is given in table 1. The number and strength of acid sites of the modified aluminas do not change significantly relative to the starting material. Thus, the changes in the alumina acidity with loading 1 wt.% Si or 1.5 wt.% Ti can hardly explain the increased activity of Si- and Ti-doped catalysts.

3.4. Conventional XRD and BET characterization of Ti- and Si-doped aluminas and the corresponding Ag-catalysts

To investigate if Ti- and Si-doping significantly altered the crystal structure of the Ag/Al_2O_3 X-ray diffraction patterns of the catalysts and the corresponding supports were recorded (Fig. 6). When comparing the catalyst supports (gray curves) a slight increase in crystallinity could be noticed (also represented by the crystal size change in table 1). An increase in the crystal size is in line with the decreased surface area S_{BET} of the doped aluminas (table 1).

Comparison of the XRD spectra of Ag/Al_2O_3 (black curves in Fig. 6) catalysts shows a noticeable difference between the undoped reference Ag/Al_2O_3 and doped Ag/1.5Ti/Al_2O_3 and Ag/1Si/Al_2O_3. There are clear reflections arising from metallic Ag in the reference sample spectrum (2θ angles = 38.1, 44.3, 64.5, 77.4, and 81.5°). None of these silver reflections can be found in the spectra of doped catalysts suggesting very small and dispersed Ag particles.

3.5. Synchrotron XRD, EXAFS and XAS-TPR study of Ag/Siralox in comparison to Ag/Al_2O_3-noSO_x

To obtain better quality XRD patterns and to complement these data with XAS results we have conducted in-situ XAS-TPR using high brilliant synchrotron X-rays. The catalysts were placed in the quartz capillary used as an in-situ cell with a flow of 5% H_2/He. After 3 min in the reducing atomsphere XRD scans were recorded, followed by 5 EXAFS scans (approx. 3 min each) at 20 °C and continuous recording of EXAFS spectra during subsequent heating. After reaching 480 °C the catalysts were cooled in H_2/He flow to 30 °C and XRD patterns and EXAFS spectra were recorded once again. In-situ XAS-TPR was chosen as a characterization technique because Ag/Al_2O_3 catalysts undergo reduction (necessary for particle size estimation [28]) not under in-situ SCR conditions but only in more reducing atmospheres, as also observed by Shimizu et al. [29].

Fig. 7 shows the result of linear combination analysis of XANES spectra obtained during TPR of Ag/Siralox and Ag/Al_2O_3-noSO_x catalysts. Unsulfated Ag/Al_2O_3-noSO_x was chosen for this experiment to match Ag/Siralox which was originally not presulfated. The value displayed on Y-axis in Fig. 7 is the relative fraction of Ag^0 (relative contribution of XANES spectrum of the reduced catalyst to the resulting spectra). The error bars reflect the goodness of the fit. Original XANES spectra are available in the supporting material. First and last EXAFS spectra of the same catalyst were used as standards for fitting representing Ag^+ and Ag^0 respectively. The reason for not using the spectra of reference compounds (see supporting material) is that they are obtained using highly crystalline materials and show higher amplitude of EXAFS oscillations than the spectra of the catalysts which results in a bad fit.

As shown in Fig. 7, reduction of Ag/Al_2O_3-noSO_x starts immediately upon exposure to H_2/He at 20 °C (first 5 points, black line). This is not the case for Ag/Siralox (gray

line) where higher temperature is needed for reduction of Ag species. Shift of Ag reduction to lower temperatures have been observed previously with increase of Ag content and was ascribed to a formation of bigger Ag_xO_y clusters [30]. Alternatively, easier reduction of undoped Ag/Al_2O_3-noSO_x may be due to lower metal-support interaction.

XRD patterns of the oxidized catalysts (Fig. 8) show intense broad signals of γ-Al_2O_3 with small sharp signals from metallic Ag and, possibly, Ag_2O [31]. The inset in the top left corner shows enlarged signals with subtracted baseline at 2θ = 12.3° (reflections from Ag 1 1 1 and Ag_2O 2 0 0 crystal planes) and 2θ = 23.7° (Ag 3 1 1). Higher intensity of Ag and Ag_2O signals points to a larger crystal size of Ag particles in the case of Ag/Al_2O_3-noSO_x relative to Ag/Siralox.

Fourier transformed EXAFS (first scan at 20 °C) spectra of Ag/Siralox and Ag/Al_2O_3-noSO_x catalysts are shown in Fig. 9. In line with the XRD data, stronger metallic features (backscattering from the neighboring Ag at R = 2.7 Å, no phase correction) for the Ag/Al_2O_3-noSO_x is observed relative to Ag/Siralox. The latter, in turn, shows higher intensity from the oxygen backscatterer at lower R-values and is, therefore, more oxidized. Note that these spectra were measured already in the presence of H_2 and, strictly speaking, the state of a catalyst present in the beginning of TPR may be different from the catalyst in air. This could be important in the case of Ag/Al_2O_3-noSO_x which showed reduction already at 20 °C.

XRD and EXAFS spectra of the reduced catalysts (not presented here, see the supporting material) are identical and dominated by signals from metallic Ag indicating that TPR completely redistributes Ag species to form metallic Ag of similar size and shape independent on the support properties.

4. Discussion

Among the different catalysts used in this study Ag/Al_2O_3 doped with small amounts of Ti and Si demonstrate higher catalytic activity at low temperatures (after degreening with SO_2). However, they are more prone to deactivation by sulfur compounds during H_2-assisted SCR of NO_x by ammonia. To explain these phenomena we employed further test studies and several characterisation techniques. Loading of Ti and Si did not increase the acidity of the alumina support. The changes in the acidity of the doped aluminas can probably not be seen due to the low amounts of dopants in the most active catalysts.

The surface area of the doped supports (table 1) is decreased by 10 – 15% relative to the reference alumina. The decrease in surface area after introduction of low amounts of Si and Ti in alumina has been reported earlier [16, 27].

The most prominent difference between the undoped catalyst and its doped analogues can be noticed in the conventional XRD patterns and in the results of the synchrotron X-ray diffraction and X-ray absorption study. The diffractogram of the reference catalyst shows reflections originating from metallic Ag particles, whereas no Ag species could be detected in the spectra of doped samples suggesting better Ag dispersion in these catalysts. A similar observation was found by Li at al. [15] – in that case for HC SCR. The lower Ag dispersion in the undoped catalyst can also be indirectly concluded from the reduction in $5\%H_2$/He followed by X-ray absorption spectroscopy as the undoped catalyst reduces easier already at room temperature (see e.g. similar studies on Pd-based catalysts [32]).

Indeed, doped aluminas in our case have a relatively constant total amount of acid sites in spite of the decreasing surface area. This gives higher surface density of acid sites for the doped samples, thus, providing more nucleation sites for active Ag particles per surface area. Hence, Ag is utilized more efficiently and the metal-support interaction is stronger in this case preventing Ag species from agglomeration. This fact also explains why the effect of doping is only observed if Ag is loaded on Ti-doped support but not if already prepared Ag/Al_2O_3 is later doped with Ti. In the second case we tried to modify a prepared catalyst with already formed Ag particles which did not lead to the enhancement of the catalytic properties.

The second effect of Ti and Si doping is the modification of the catalyst affinity towards SO_x influencing catalyst deactivation and regeneration properties. Several authors reported lower stability of sulfates on TiO_2 and SiO_2 relative to the alumina [15, 16, 33] which was also confirmed during our catalytic tests. Fig. 10 shows the amount of SO_2 desorbed during the first (top) and the sixth (bottom) regeneration stages in the course of catalyst degreening in dependence on the Si or Ti loading. These two regeneration stages are chosen to indicate the initial sulfur uptake by the just-prepared catalysts and sulfur adsorption-desorption during the "steady-state" operation of the degreened catalyst. Two different trends are present. In the case of the freshly presulfated catalyst subjected to the regeneration $Ag/1.5Ti/Al_2O_3$ desorbes nearly three times the amount of SO_2 as the reference Ag/Al_2O_3 and this amount increases with the increase in the dopant loading. At the same time, degreened catalysts adsorb and desorb comparable amounts of SO_2 ($Ag/1.5Ti/Al_2O_3$ stores and releases approx. 1.3 times more SO_2 than the undoped sample). Altogether, the dopant influences stronger the catalyst preparation and the degreening stage than the further catalyst operation.

In spite of the comparable amount of the desorbed SO_2 during operation of the degreened catalyst desorption temperatures differ. Fig. 11 shows evolution of SO_2 from $Ag/1.5Ti/Al_2O_3$ (black solid) and $Ag/1Si/Al_2O_3$ (black dashed) as well as from the undoped Ag/Al_2O_3 (gray solid) in the course of catalyst regeneration under SCR conditions. Addition of Ti and Si to the catalyst resulted in SO_2 desorption to the gas phase at lower temperatures during the catalyst regeneration compared to the undoped Ag/Al_2O_3 which supports the idea of more efficient regeneration of Ti- and Si-doped Ag/Al_2O_3 catalysts. Moreover, two SO_2 desorption peaks are observed in the case of $Ag/1.5Ti/Al_2O_3$ suggesting different types and configuration of sites for adsorption of sulfur species in the case of doped catalysts.

The obtained data allows to draw the mechanism of Ag/Al_2O_3 doping is as follows: First, doping of Ag/Al_2O_3 leads to the formation of smaller Ag particles, i.e. better Ag dispersion. The smaller active Ag particles explain faster deactivation during SO_2 exposure for Ti-doped catalysts compared to the undoped Ag/Al_2O_3 as smaller Ag particles are known to be less stable towards sulfur poisoning [12, 18, 19]. Second, as seen from the amount of SO_2 desorbed after the first regeneration, the amount of SO_2 irreversibly adsorbed on the doped catalysts is lower which leaves less Ag sites irreversibly poisoned and accessible for the SCR [18] in the degreened catalyst. And last, in spite of adsorbing more sulfur species during the degreened catalyst operation, those species are, bound weaker than to the undoped catalyst and easily desorbed during regeneration.

The changes in the strength and, possibly, the nature of surface adsorption sites can influence not only adsorption of SO_2 but also NO_x and NH_3 and, thus, account for the existence of optimum Ti and Si loadings as seen in the Fig. 3. While the initial increase

of the catalytic activity stems from the better Ag dispersion, further decrease can be a result of changes in the strength and, probably, geometry of various adsorption sites (e.g. those adsorbing nitrate and nitrite intermediates [34]). Further insight about this could probably be obtained using in-situ DRIFTS spectroscopy.

Last but not least, the activity of the catalysts based on the laboratory doped alumina was compared with that of Ag supported on commercial silica-aluminas prepared by co-precipitation. The results demonstrate the same effect of doping by Si in this case, though the concentration of Si required for the production of the most active catalyst is higher in the case of co-precipitated silica-aluminas. This probably stems from the fact that by impregnating the support we introduce the dopant mainly on the surface, whereas co-precipitation yields dopant uniformly distrubuted in the bulk. Thus, a relatively higher surface concentrations are obtained in the first case. As the catalytic effect is governed by the surface sites the required amount of the dopant will be lower if introducing it via impregnation. Still, as Si and Ti are cheap and readily available, the usage of commercial co-precipitated supports is justified by the easyness of the preparation and, correspondently, the end price of the catalyst.

5. Conclusions

Doping alumina support of the Ag/Al_2O_3 catalysts by low amounts of Ti and Si allows gaining higher low-temperature activity of the catalysts in the H_2-assisted SCR of NO_x by NH_3 under sulfating conditions. From the detailed characterization we conclude that this can be mainly traced back to better Ag dispersion in the doped samples together with the more efficient regeneration of the obtained catalysts from sulfur. The optimum dopant loading is about 1 – 1.5 wt.% and according to the various

preparation methods and supports used in the study the findings can be extended to the usage of commercial co-precipitated silica-aluminas. In this case the optimal concentration of the dopant will be higher, e.g. 3% Si compared to 1% Si for the alumina doped by impregnation.

6. Acknowledgments

This work was supported by the grant 09-067233 from The Danish Council for Strategic Research. The authors also want to thank SASOL Germany for kindly providing the commercial silica-alumina. We acknowledge the European Synchrotron Radiation Facility for providing beam time and financial support, the BMBF-project "Materials in Action" for financial support of in situ XAS studies and, finally, we would like to thank Dr. Wouter van Beek for his assistance in using beamline BM01B and the corresponding infrastructure. We also thank Dr. Hudson W.P. de Carvalho, Dipl.Chem. Andreas M. Gänzler, and Dr. Henning Lichtenberg for the assistance during the beam time.

References

[1] F. Klingstedt, K. Eränen, L.-E. Lindfors, S. Andersson, L. Cider, C. Landberg, E. Jobson, L. Eriksson, T. Ilkenhans, D. Webster , Top. Catal. 30/31 (2004) 27-30

[2] T.V. Johnson, Int. J. Engine Res. 10 (2009) 275-285

[3] K.M. Adams, J.V. Cavataio, R.H. Hammerle, Appl. Catal. B 10 (1996) 157-181

[4] D.W. Fickel, E. D'Addio, J.A. Lauterbach, R.F. Lobo, Appl. Catal. B 102 (2011) 441-448

[5] S. Matsumoto, Catal. Today 29 (1996) 43-45

[6] M. Weibel, N. Waldbüßer, R. Wunsch, D. Chatterjee, B. Bandl-Konrad, B. Krutzsch, Top. Catal. 52 (2009) 1702-1708

[7] G. Madia, M. Koebel, M. Elsener, A. Wokaun, Ind. Eng. Chem. Res. 41 (2002) 3512-3517

[8] A. Grossale, I. Nova, E. Tronconi, D. Chatterjee, M. Weibel, J. Catal. 256 (2008) 312-322

[9] M. Richter, R. Fricke, R. Eckelt, Catal. Lett. 94 (2004) 115-118

[10] K.-I. Shimizu and A. Satsuma, Appl. Catal. B 77 (2007) 202-205

[11] A. Abe, N. Aoyama, S. Sumiya, N. Kakuta, K. Yoshida, Catal. Lett. 51(1998) 5-9

[12] P.W. Park and C.L. Boyer, Appl. Catal. B 59 (2005) 27–34

[13] P.A. Kumar, M.P. Reddy, B. Hyun-Sook, H.H. Phil, Catal. Lett. 131 (2009) 85-97

[14] L. Valanidou, C. Theologides, A.A. Zorpas, P.G. Savva, C.N. Costa, Appl. Catal. B 107 (2011) 164-176

[15] J. Li, Y. Zhu, R. Ke, J. Hao, Appl. Catal. B 80 (2008) 202-213

[16] N. Jagtap, S.B. Umbarkar, P. Miquel, P. Granger, M.K. Dongare, Appl. Catal. B 90 (2009) 416-425

[17] M. Richter, U. Bentrup, R. Eckelt, M. Schneider, M.-M. Pohl, R. Fricke, Appl. Catal. B 51 (2004) 261-274

[18] D.E. Doronkin, T.S. Khan, T. Bligaard, S. Fogel, P. Gabrielsson, S. Dahl, Appl. Catal. B 117-118 (2012) 49–58

[19] S. Fogel, D.E. Doronkin, P. Gabrielsson, S. Dahl, Appl. Catal. B 125 (2012) 457–464

[20] J.-D. Grunwaldt, M. Caravati, S. Hannemann, A. Baiker, PCCP 6 (2004) 3037-3047

[21] J.-D. Grunwaldt, N. van Vegten, A. Baiker, Chem. Commun. (2007) 4635.

[22] W. van Beek, O.V. Safonova, G. Wiker, H. Emerich, Phase Transitions 84 (2011) 726-732

[23] A.P. Hammersley, S.O. Svensson, M. Hanfland, A.N. Fitch, D. Häusermann, High Pressure Research 14 (1996), 235-248

[24] B. Ravel, M. Newville, J. Synchrotron Radiat. 12 (2005) 537-541

[25] B. Greenhalgh, M. Fee, A. Dobri, J. Moir, R. Burich, J.-P. Charland, M. Stanciulescu, J. Mol. Catal. A 333 (2010) 121–127

[26] P. Padmaja, K.G.K. Warrier, M. Padmanabhan, W. Wunderlich, J. Sol-Gel Sci. Technol. 52 (2009) 88–96

[27] B. Schimmoeller, F. Hoxha, T. Mallat, F. Krumeich, S.E. Pratsinis, A. Baiker, Appl. Catal. A 374 (2010) 48–57

[28] K.-i. Shimizu, M. Tsuzuki, K. Kato, S. Yokota, K. Okumura, A. Satsuma, J. Phys. Chem. C 111 (2007) 950-959

[29] J.P. Breen, R. Burch, C. Hardacre, C.J. Hill, J. Phys. Chem. B, 109 (2005) 4805-4807

[30] C. Petitto, P.H. Mutin, G. Delahay, Top. Catal. 56 (2013) 34-39

[31] R.-S. Zhou, R.L. Snyder, Acta Crystallographica B 47 (1991) 617-630; H.E. Swanson, E. Tatge, National Bureau of Standards (U.S.), Circular 539 (1953), 1-95;

T. Suzuki, Journal of the Physical Society of Japan 15 (1960) 2018-2024. Cited via ICSD (FIZ Karlsruhe).

[32] J.-D. Grunwaldt, B. Kimmerle, S. Hannemann, A. Baiker, P. Boye, C.G. Schroer, J. Mater. Chem. 17 (2007), 2603- 2606

[33] Z. Liu, J. Li, A.S.M. Junaid, Cat. Today 153 (2010) 95-102

[34] D.E. Doronkin, S. Fogel, S. Tamm, L. Olsson, T.S. Khan, T. Bligaard, P. Gabrielsson, S. Dahl, Appl. Catal. B 113-114 (2012) 228-236

Table 1. Textural characteristics of used alumina and Ti (Si)-alumina supports.

Support	Support BET surface area, [m^2/g]	Average crystallite size, [Å]	Number of acid sites, [mmol/g]
Al_2O_3	298	34	0.55
1.5%Ti-Al_2O_3	276	37	0.57
1%Si-Al_2O_3	253	63	0.51
Siralox 5/230	292	-	-

Figure legends

Figure 1. NO_x conversion profiles obtained over reference Ag/Al_2O_3 (black solid line), $Ag/1.5Ti/Al_2O_3$ (black dashed line), $Ag/1Si/Al_2O_3$ (black dotted line), Ag/Siralox (gray dotted line), $Ag/1Mg/Al_2O_3$ (gray solid line), and over $Ag/1W/Al_2O_3$ (gray dashed line). Reaction conditions: 500 ppm NO, 520 ppm NH_3, 1200 ppm H_2, 8.3% O_2, 7% H_2O in Ar, GHSV = 110 000 h^{-1}.

Figure 2. Decrease of NO_x conversion during feeding SO_2 at 250 °C over Ag/Al_2O_3 (black solid line), $Ag/1.5Ti/Al_2O_3$ (black dashed line), $Ag/1Si/Al_2O_3$ (black dotted line), Ag/Siralox (gray dotted line), and $Ag/1Mg/Al_2O_3$ (gray solid line). Reaction conditions: 10 ppm SO_2, 500 ppm NO, 520 ppm NH_3, 1200 ppm H_2, 8.3% O_2, 7% H_2O in Ar, GHSV = 110 000 h^{-1}.

Figure 3. Dependence of temperature of 50% NO_x conversion on dopant loading for $Ag/xTi/Al_2O_3$ (solid line) and $Ag/xSi/Al_2O_3$ (dashed line). Reaction conditions: 500 ppm NO, 520 ppm NH_3, 1200 ppm H_2, 8.3% O_2, 7% H_2O in Ar, GHSV = 110 000 h^{-1}.

Figure 4. Dependence of NO_x conversion after 2 h exposure to 10 ppm SO_2 on dopant loading for $Ag/xTi/Al_2O_3$ (solid line) and $Ag/xSi/Al_2O_3$ (dashed line). Reaction conditions: 10 ppm SO_2, 500 ppm NO, 520 ppm NH_3, 1200 ppm H_2, 8.3% O_2, 7% H_2O in Ar, GHSV = 110 000 h^{-1}.

Figure 5. NH_3 TPD profiles for unsulfated $1.5Ti/Al_2O_3$ (dashed), $1Si/Al_2O_3$ (dotted), and reference Al_2O_3 (solid). Conditions: 100 mg. of sample, 100 ml/min Ar flow, 5 °/min temperature ramp.

Figure 6. XRD spectra of $Ag/1.5Ti/Al_2O_3$, $Ag/1Si/Al_2O_3$, Ag/Al_2O_3 catalysts (black), and the corresponding supports (gray).

Figure 7. Results of linear combination fitting of XANES spectra obtained during temperature-programmed reduction of Ag/Siralox (gray) and Ag/Al_2O_3-noSO_x (black). Showed value is the concentration of Ag^0 relative to the total concentration of Ag in the catalyst (weight of the spectrum of the reduced catalyst).

Figure 8. Synchrotron-XRD spectra of of Ag/Siralox (gray) and Ag/Al_2O_3-noSO_x (black) before TPR. X-ray wavelength $\lambda = 0.505268$ Å. Inset shows peaks near $2\theta = 12.3°$ and $2\theta = 23.7°$ with subtracted linear baseline.

Figure 9. Fourier transformed EXAFS spectra (first scan) of Ag/Siralox and Ag/Al_2O_3-noSO_x with Ag and Ag_2O reference spectra.

Figure 10. Amount of SO_2 desorbed from $Ag/xTi/Al_2O_3$ (filled circles) and $Ag/xSi/Al_2O_3$ (open triangles) catalysts during the first (top) and the sixth (bottom) regeneration stages in the course of catalyst degreening depending on the amount of Si and Ti. Amount of SO_2 passing through the catalyst during each deactivation cycle is 5.9 μmol.

Figure 11. SO_2 concentration in catalyst outlet during degreening (incl. the sixth regeneration stage) of Ag/Al_2O_3 (gray solid line), $Ag/1.5Ti/Al_2O_3$ (black solid line), $Ag/1Si/Al_2O_3$ (black dashed line). Catalyst temperature is plotted as gray dashed line.

Figure 1.

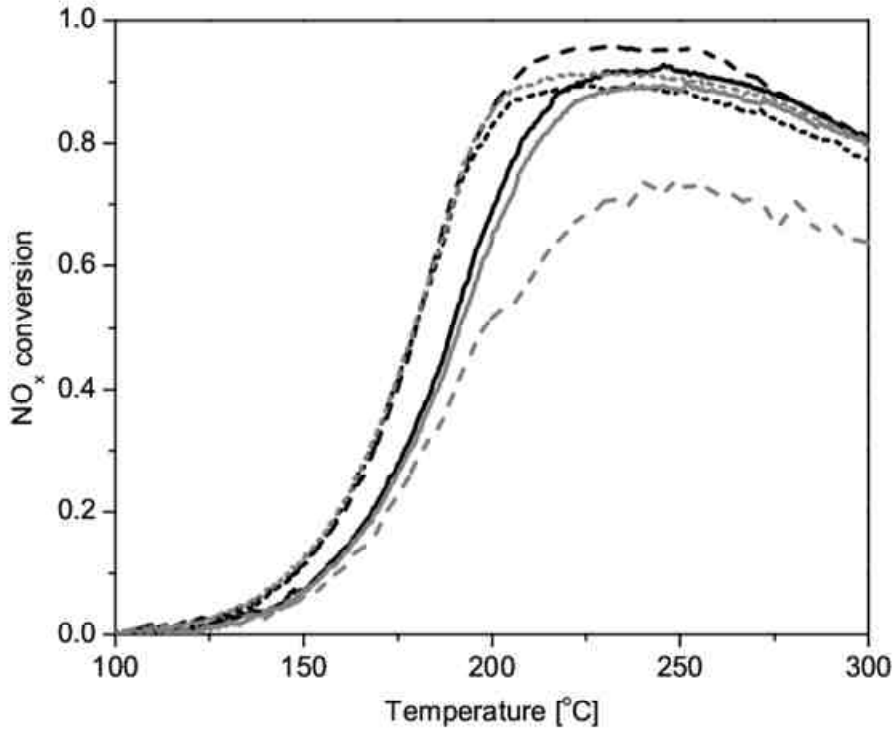
1.0
0.8
0.6
0.4
0.2
0.0
NOx conversion
100
150
200
250
300
Temperature [°C]

Figure 2.

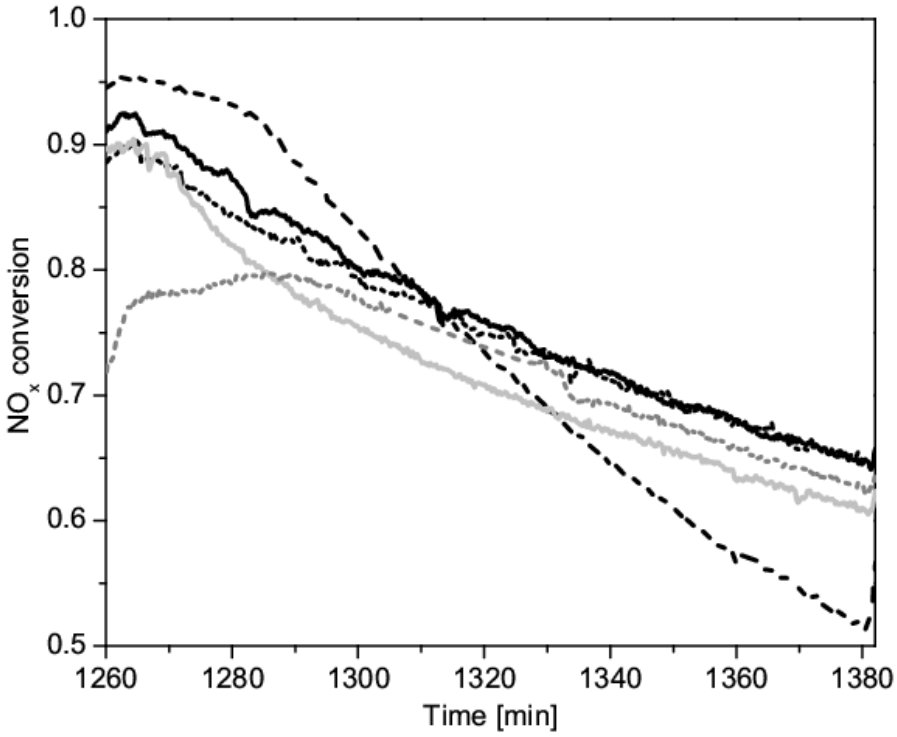
1.0
0.9
0.8
0.7
0.6
0.5
NOx conversion
1260
1280
1300
1320
1340
1360
1380
Time [min]

Figure 3.

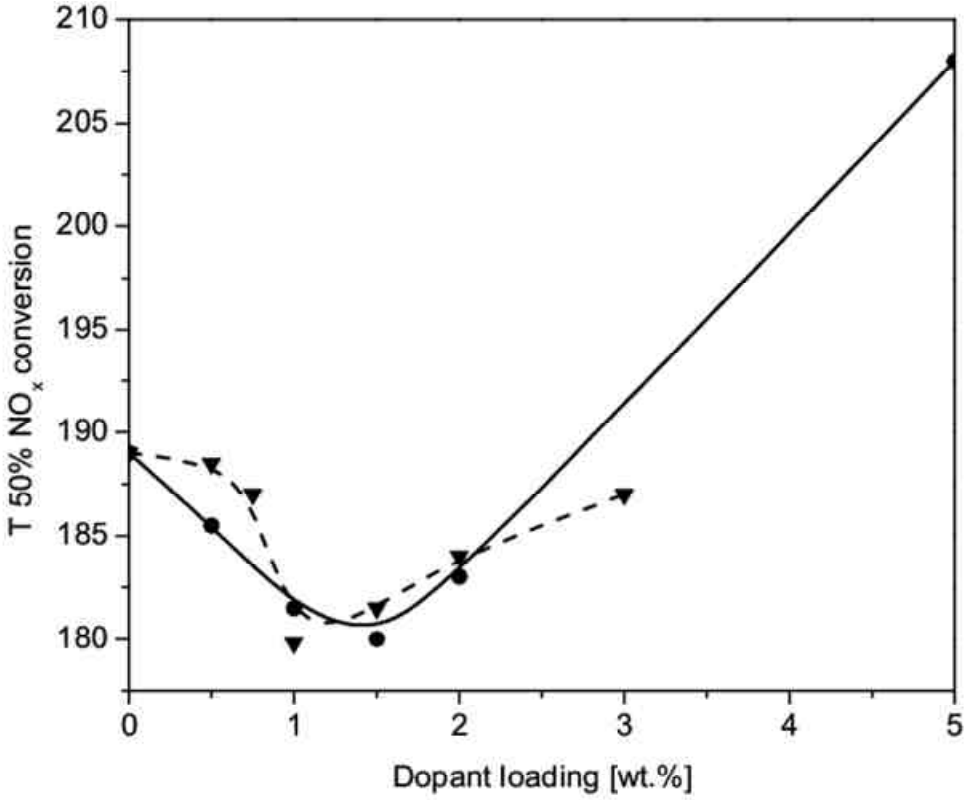
T 50% NOx conversion
Dopant loading [wt.%]
210
205
200
195
190
185
180
0
1
2
3
4
5

Figure 4.

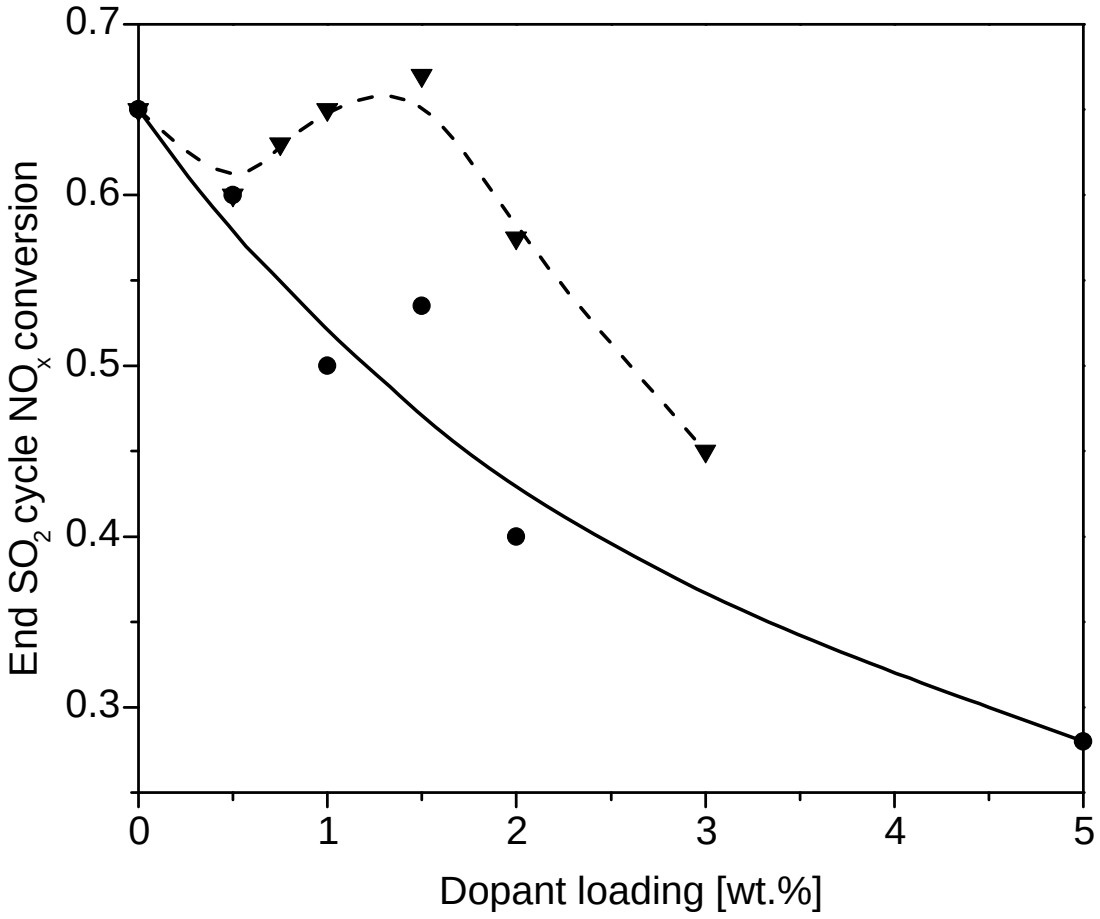
0.7
0.6
0.5
0.4
0.3
End SO_2 cycle NO_x conversion
0
1
2
3
4
5
Dopant loading [wt.%]

Figure 5.

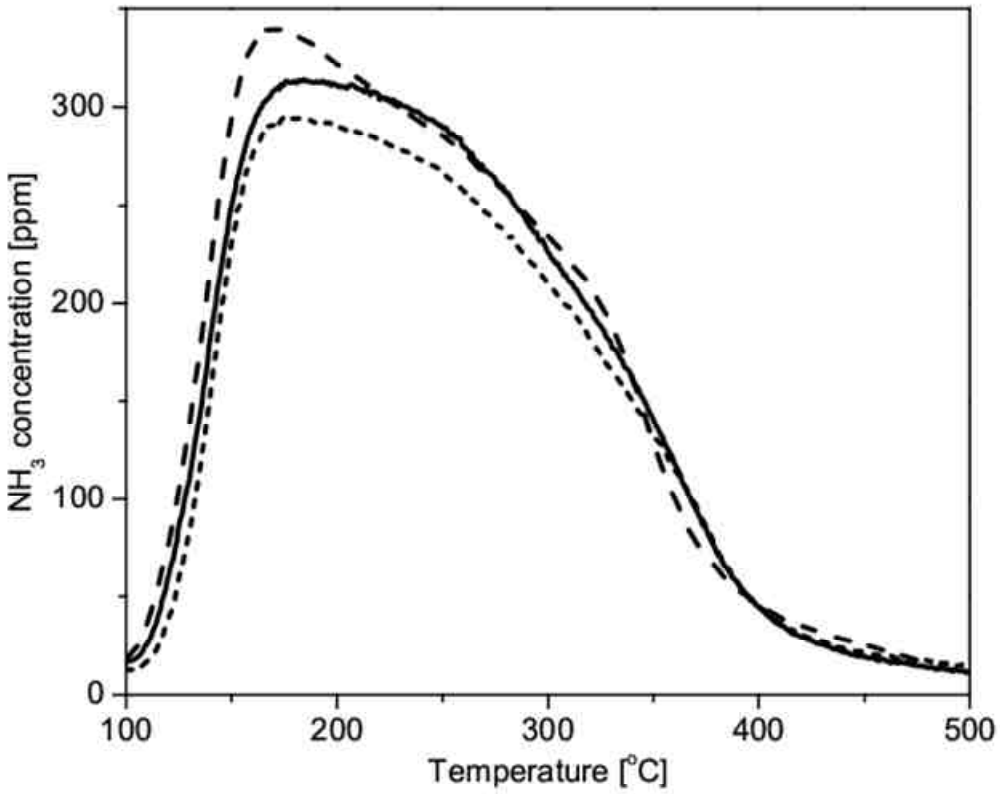
300
200
100
0
NH3 concentration [ppm]
100
200
300
400
500
Temperature [°C]

Figure 6.

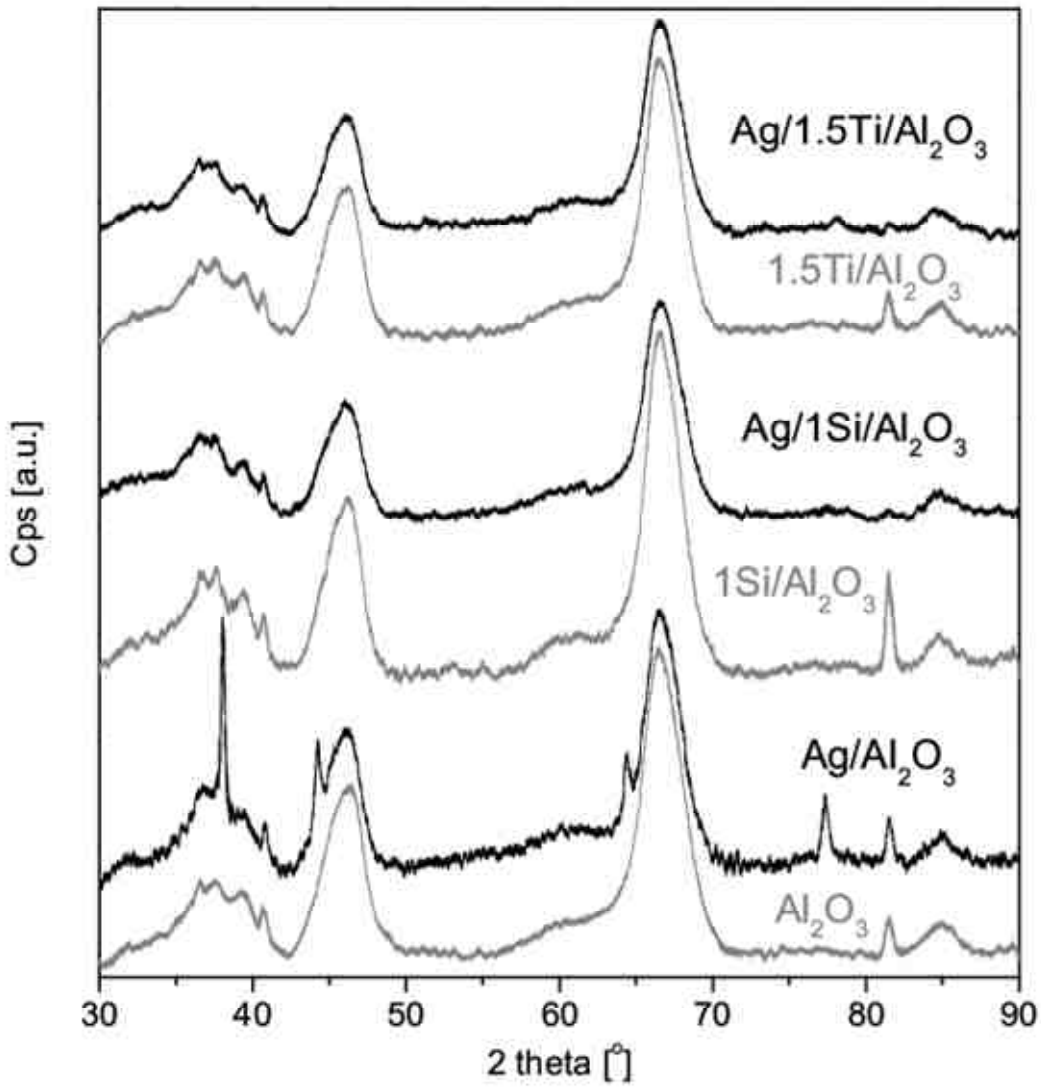
Ag/1.5Ti/Al2O3
1.5Ti/Al2O3
Ag/1Si/Al2O3
1Si/Al2O3
Ag/Al2O3
Al2O3
Cps [a.u.]
30
40
50
60
70
80
90
2 theta [°]

Figure 7.

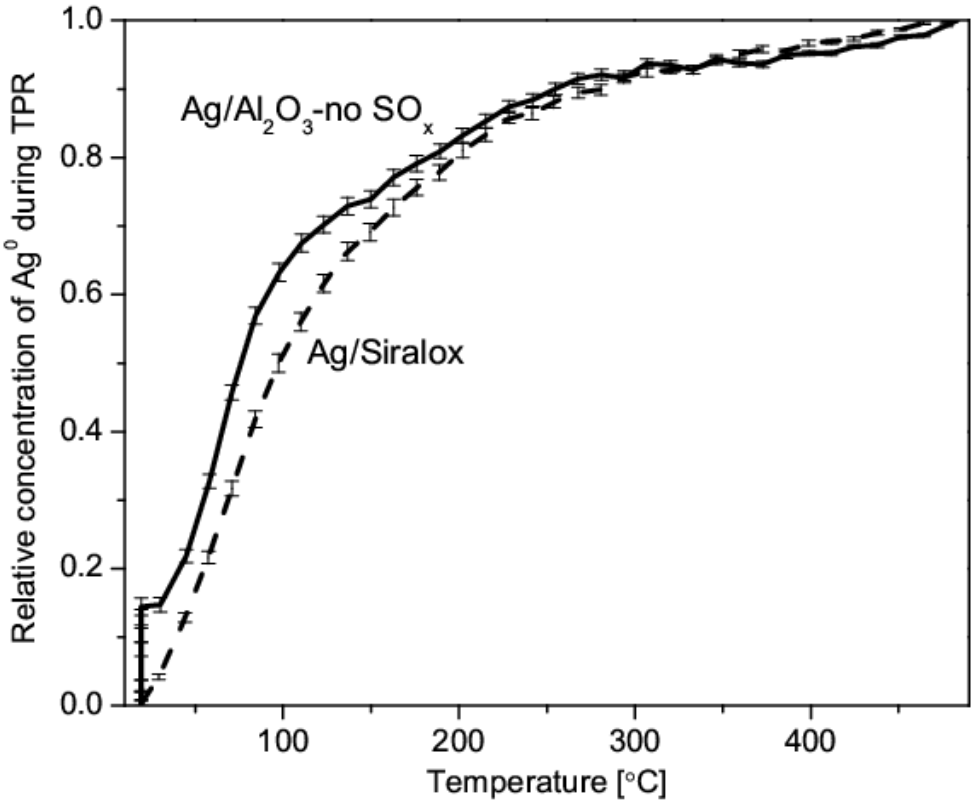
Relative concentration of Ag^0 during TPR
Temperature [°C]
Ag/Al$_2$O$_3$-no SO$_x$
Ag/Siralox
0.0
0.2
0.4
0.6
0.8
1.0
100
200
300
400

Figure 8.

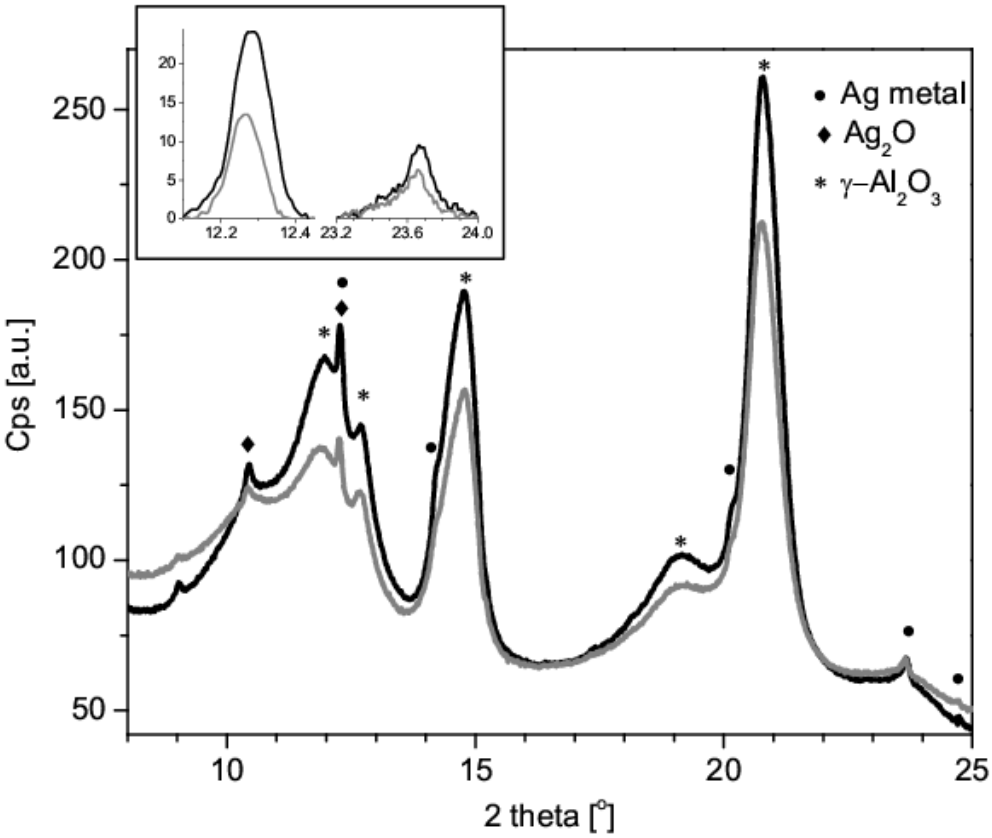
Ag metal
Ag2O
γ–Al2O3
Cps [a.u.]
2 theta [°]
250
200
150
100
50
10
15
20
25
20
15
10
5
0
12.2
12.4
23.2
23.6
24.0

Figure 9.

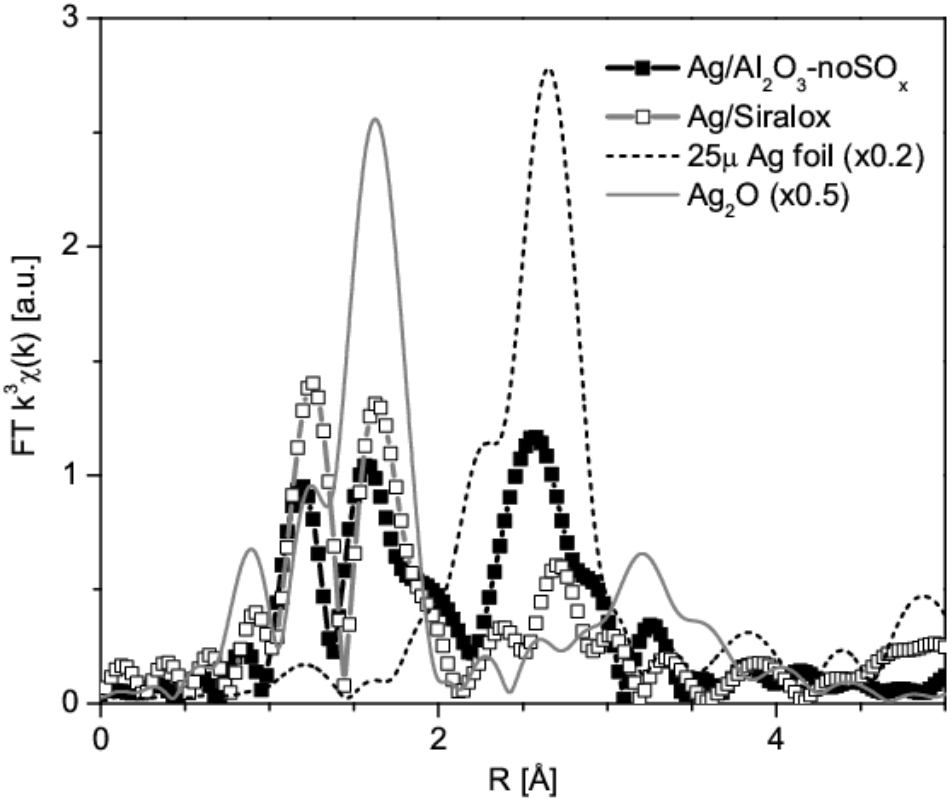
Ag/Al2O3-noSOx
Ag/Siralox
25μ Ag foil (x0.2)
Ag2O (x0.5)
FT k3χ(k) [a.u.]
R [Å]
0
1
2
3
0
2
4

Figure 10.

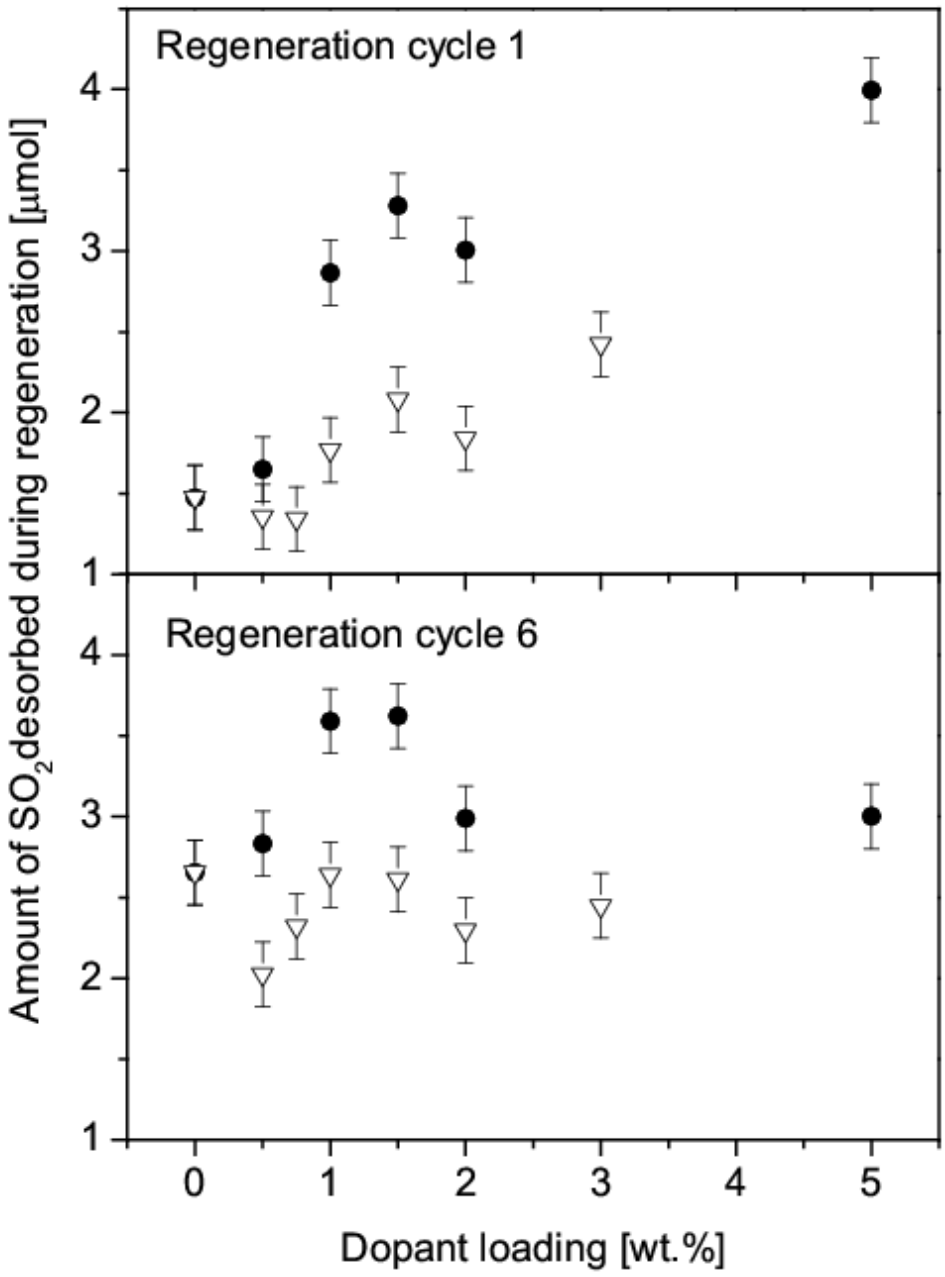
Regeneration cycle 1
Regeneration cycle 6
Amount of SO_2 desorbed during regeneration [µmol]
Dopant loading [wt.%]
1
2
3
4
0
1
2
3
4
5

Figure 11.

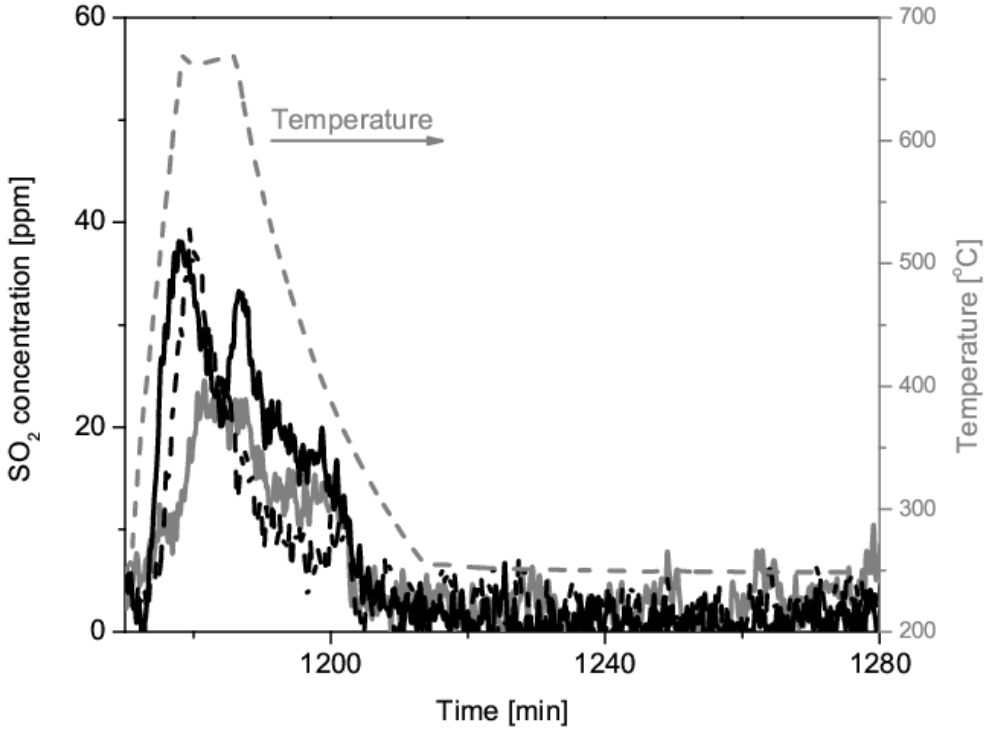
60
40
20
0
700
600
500
400
300
200
Temperature
SO2 concentration [ppm]
Temperature [°C]
1200
1240
1280
Time [min]